

SUPPLEMENTARY INFORMATION

Handheld Isothermal Amplification and Electrochemical Detection of DNA in Resource-Limited Settings

Tsaloglou, M-N., Nemiroski.A., Camci-Unal.G., Christodouleas.D.C., Murray.L.P., Connelly.J.T., and Whitesides..G.M.

Supporting Introduction

We used the RPA reaction for DNA amplification (Figure SI 1); we chose RPA because the cost and complexity of the components for thermoregulation is lower than those required by PCR. Other commonly used isothermal methods include loop-mediated isothermal amplification (LAMP),^[1] nucleic acid sequence-based amplification (NASBA)^[2] and helicase dependent amplification (HDA).^[3]

We designed and fabricated a paper-based test strip that included the ceramic substrate and layers of tape and paper. The methods of fabrication of the paper-based strips are described in page 5 of the supplementary information section. We first evaluated the effect of the paper layer on the electrochemical performance of the redox probe. Figure SI 6 shows SWVs for the same concentration of the redox probe on the disposable paper-based test strip *vs.* a liquid droplet on the ceramic substrate measured by the uMED^{NA}. We observed that using the paper matrix reduces the amplitude of the anodic peak by approximately 24%, compared to the case of the liquid droplet of the same volume. Diffusion of a chemical species in solution is governed by a concentration gradient in accordance with Fick's law, where D_0 is the diffusion coefficient; the maximum current in SWV is proportional to the square root of D_0 .^[4] We expect that the rate of diffusion would be slower in a porous matrix such as paper mainly because of (i) a reduced cross-sectional area of diffusion to the electrodes in paper, and (ii) more tortuous pathways for

diffusion to the electrodes, compared to a homogeneous liquid droplet.^[5] Others have observed similar behavior for electrochemical measurements in paper^[6], soil,^[7] and hydrogels.^[8]

Supporting Methods

Cell Cultures

M. smegmatis strain ATCC 700084 was purchased from the American Type Culture Collection (ATCC, Virginia, USA) as a lyophilized pellet. The pellet was rehydrated in sterile 7H9 broth base. The broth base consisted of 5 g/L Middlebrook 7H9 solid broth base, 0.2% (v/v) glycerol, 10% (v/v) albumin dextrose catalase Middlebrook growth supplement (ADC), 1 mM CaCl₂, 50 µg/mL carbenecillin and 10 µg/mL cycloheximide. An aliquot of the cell suspension was spotted onto a 7H10 agar plate and grown in a static incubator (C24, New Brunswick Scientific, Connecticut, USA) at 37 °C for four days until colonies formed. Each 7H10 agar plate consisted of 10 mL of a sterile solidified solution of 20 g/L 7H10 agar powder, 0.5% (v/v) glycerol, 10% (v/v) oleic acid albumin dextrose catalase Middlebrook growth supplement (OADC), 1 mM CaCl₂, 50 µg/mL carbenecillin and 10 µg/mL cycloheximide. One colony from the agar plate was inoculated into 50 mL of 7H9 broth base enriched with 0.05% (v/v) Tween 80. The culture was grown in an incubator shaker (C24, New Brunswick Scientific, Connecticut, USA) at 37 °C for three days. Finally, an aliquot (1 mL) of this culture was used to inoculate 50 mL of the 7H9 broth base and the resulting solution was grown in an incubator shaker at 37 °C overnight. The following day, the culture was used for DNA extraction and purification.

Cell Lysis and DNA Extraction

We lysed an aliquot (2 mL) of the *M. smegmatis* cell culture using a custom-made lysis buffer for Gram-positive bacteria (20 mM Tris-HCl, 2 mM sodium EDTA, 1.2% Triton X- 100, 20 mg/mL lysozyme). Using the DNeasy kit (Qiagen, California, USA), we next extracted the DNA of the lysate following the instructions of the manufacturer. We finally eluted the purified DNA in 100 μ L of nuclease-free water (Ambion® RT-PCR Grade Water, Life Technologies, New York, USA). The yield and purity of DNA was assessed by UV-VIS spectrophotometry (Nanodrop 2000c, Thermo Scientific, New York, USA). Specifically, we used the ratio between the absorbance peaks at 260 nm and 280 nm to assess DNA purity. The intensity of the peak at 260 nm was used to estimate the yield of DNA. BEI Resources (NIAID, NIH) provided genomic DNA from *Mycobacterium tuberculosis*, strain H37Rv, NR-48669, free of charge.

Design and Validation of the Benchtop RPA Assay

To design the RPA assay, we targeted a 213-nucleotide region within the 16S rRNA sequence of genus *Mycobacterium*.^[9] Using the Primerslist open-source software, we designed the primer sequences and checked *in silico* for self- and cross-dimers.^[10] Table SI 1 lists the sequences that we used. We purchased the primers from Integrated DNA Technologies (IDT, Iowa, USA) and ran the DNA amplification reaction (RPA Basic Kit, TwistDX, Cambridge, UK) in 50- μ L reaction volumes according the instructions of the manufacturer.

To validate the RPA assay, we performed fluorescence measurements in real time on a commercial benchtop system for PCR-based detection (CFX96, Bio-Rad, Massachusetts, USA). We used SYBR Safe (1x, Life Technologies, New York, USA) as a fluorescent real-time intercalator. We performed the gold-standard, benchtop electrochemical measurements using a commercial, benchtop electrochemical analyzer (AutoLab PGSTAT12, Metrohm Florida, USA).

We performed the remainder of the electrochemical measurements on the uMED^{NA} portable device, as described in the next section. For all electrochemical RPA experiments, the standard benchtop RPA reaction was implemented with 250 μM $[\text{Ru}(\text{NH}_3)_6]\text{Cl}_3$.

Design and Fabrication of the Portable Device for Thermoregulation and Electrochemical Detection

Figure 2 describes the main components of the portable device. We fabricated an advanced version of the uMED with additional temperature control through a proportional-integral-derivative (PID) loop implemented in the Arduino programming language and executed by the same microcontroller (Atmega328, ATMEL, California, USA) that runs the uMED^{NA}. The heating subsystem consists of a flexible, resistive heating mat (0.75 mm thick, Kapton T-36067-00, Cole Parmer, Illinois, USA) powered by a high-voltage boost converter (TPS61170, Texas Instruments) to convert the 3.3 V battery supply to the voltage needed to power the heater with output current controlled by an NPN transistor (MMBT2222A-TP, Micro Commercial Components, California, USA). To tune the flow of current through the heater (and therefore, the temperature), we connected the gate of the transistor to a digital output from the microcontroller, and used pulse-width modulation to control the duty-cycle of the applied voltage. The temperature sensing subsystem consists of a temperature-to-voltage converter (MAX31855K, Maxim, California, USA) that communicates with the microcontroller by the serial-peripheral-interface protocol and is connected to the thermocouple inside the heating module through a seven-pin connector. The microcontroller uses the measured temperature as input to a software-based PID loop, and uses pulse-width modulation to adjust the temperature of the heater. Using this device, we routinely achieved ± 0.1 °C temperature stability at the set-point temperature (39.0 °C) within two minutes of initial activation of the PID control.

Design and Fabrication of the Heating Module to Interface with the Paper-based Test Strip

We designed the heating module in SolidWorks (Dassault Systèmes, Massachusetts, USA) and fabricated the components from acrylonitrile butadiene styrene (ABS) plastic by 3D printing (Fortus 250mc, Stratsys, Minnesota, USA). The base of the heating module included a slot for the test strip, as well as space for a flexible, resistive heating mat (0.75-mm thick, Kapton T-36067-00, Cole Parmer, Illinois, USA), and a seven-pin connector to mate with the uMED^{NA}. The lid contained a slot for the thermocouple (61161-372, VWR, Chicago, USA), and a three-pin modular contact (70AAJ-3-M0G, Bourns Inc., California, USA) to connect to the SPE on the test strip, when the lid was closed. The module also included space to run wires that interconnect the thermocouple, heating mat, and modular contact with the seven-pin connector. Figure SI 4 shows a circuit diagram for the heating module.

Design and Fabrication of Paper-based Test Strips

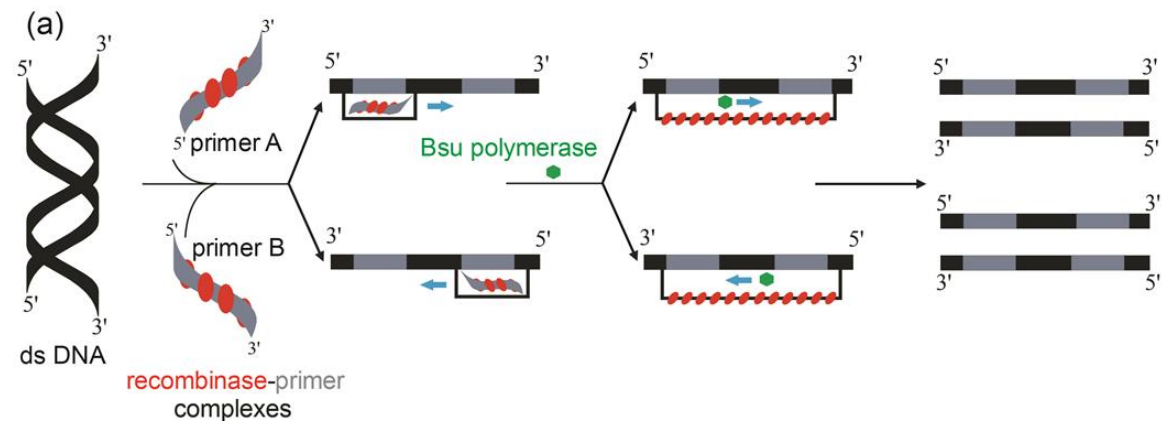
The test strips consisted of a stack of the following three components: i) a commercial, ceramic substrate with screen-printed electrodes (SPEs, DRP-110, manufactured by Dropsens (Llanera, Spain) and supplied by Metrohm, (Florida, USA))—the commercial substrate comprises three screen printed electrodes: a carbon, working electrode, a carbon, counter electrode, and a Ag/AgCl quasi-reference electrode; ii) a spacer layer formed from double-sided tape (Flexmount® Select™ DF052521, FLEXCon, New York, USA) with a 1.8-mm diameter hole cut by a laser cutter (Epilog Mini 18, Epilog Laser Systems, Colorado, USA) aligned with the electrode test area; and iii) a disposable, paper-based test strip composed of Whatman cellulose chromatography paper (1 Chr, 200 x 200 mm, Sigma Aldrich, Montana, USA) with wax barriers, printed by a Xerox ColorQube 8870W printer, defining the test zone. The spacer layer formed

from double-sided tape enabled the cellulose layer to be fastened adhesively to the ceramic electrode. Figure 2 shows the different layers of the test strip, and the ceramic substrate.

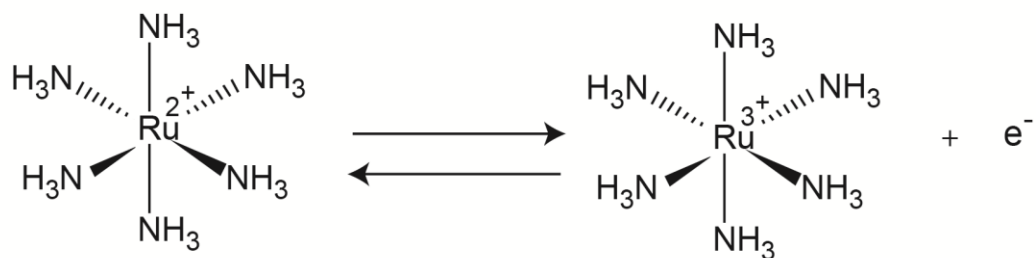
Noted that we used the rigidity of the commercial, ceramic substrate as a solid support for the entire disposable device. We disposed each ceramic substrate after each experiment, although it could be re-used if the attached layers of tape and paper are removed, and it is washed for re-conditioning. Before assembly of each complete test strip, we conditioned its component ceramic substrate by first performing a CV (0.4 to -0.4 V at 100 mV/s scan rate) of a solution of Tris-acetate buffer (40 mM, pH 7.4). We rinsed the electrodes with ultrapure deionized water and dried in a stream of N₂. The tape and paper layers were then attached on the ceramic substrate sequentially and the paper-based test strip was fabricated.

Supporting Figures

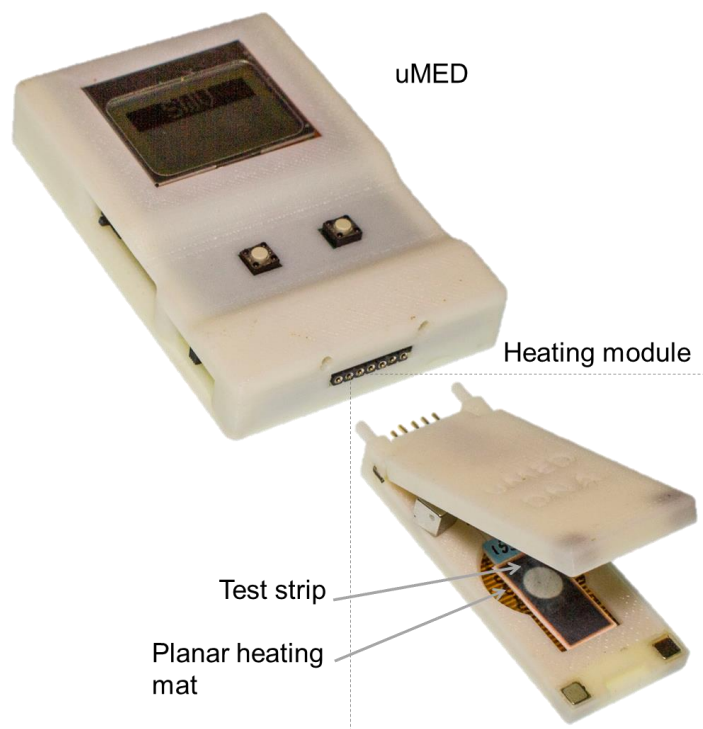
SI Figure 1: (a) Schematic representation of for the RPA reaction. Template double-stranded DNA (dsDNA) hybridizes with recombinase-primer complexes. Primers are extended by *Bacillus subtilis* (*Bsu*) polymerase in D-loop structure in the 3' direction of both strands. This process results in two copies of the original dsDNA.



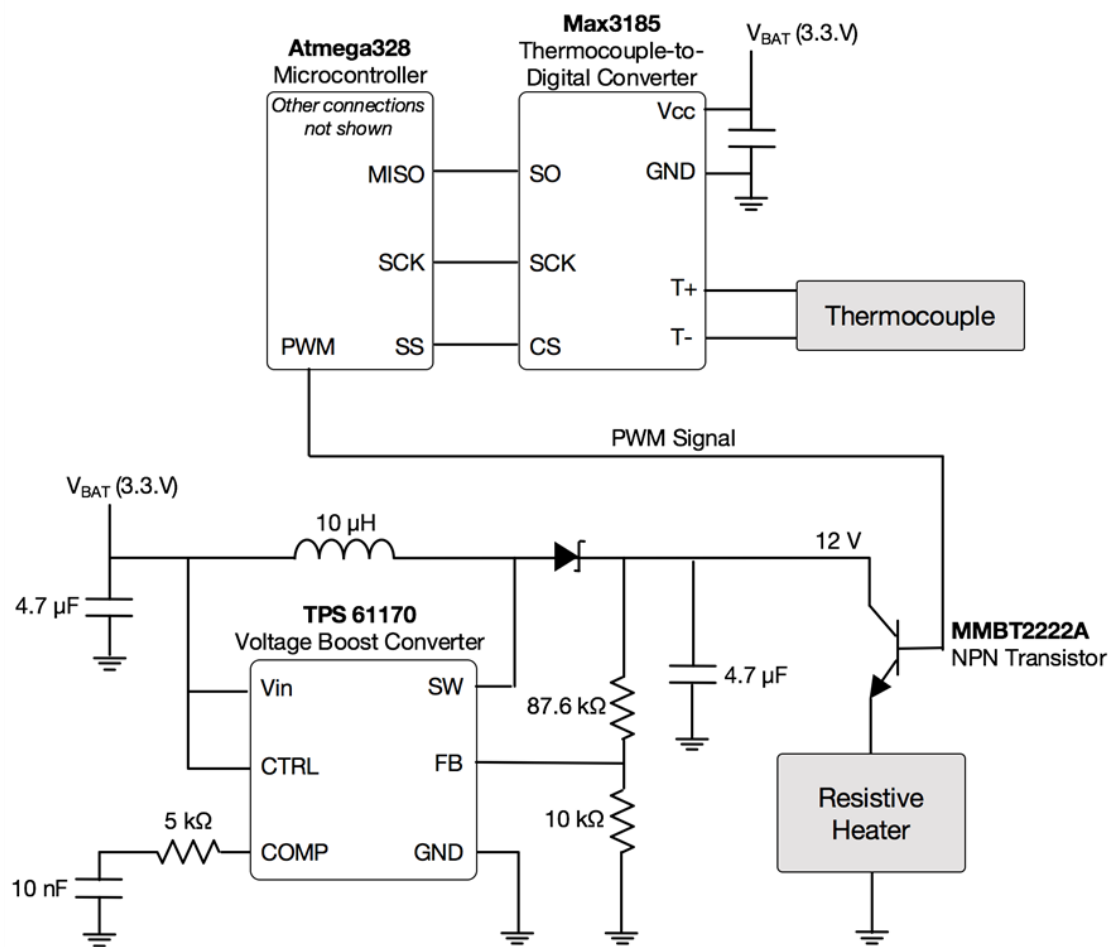
SI Figure 2: Redox couple for $[\text{Ru}(\text{NH}_3)_6]^{3+}$.



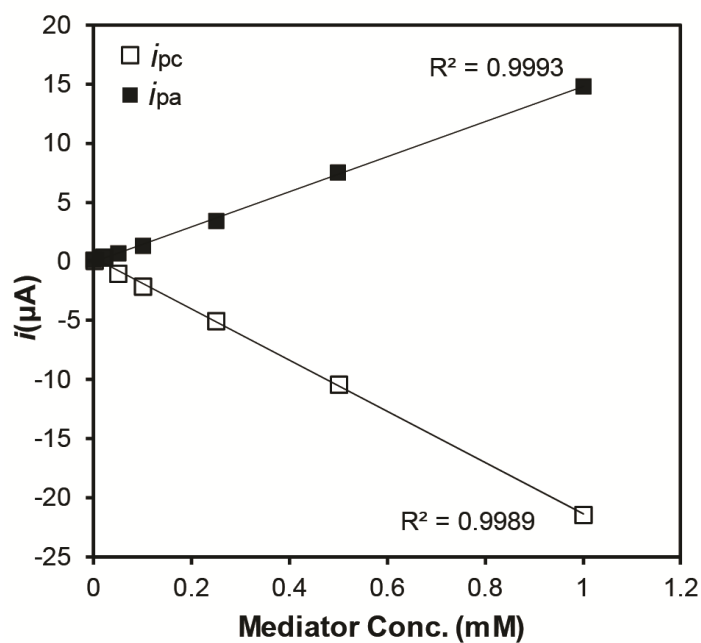
SI Figure 3: Picture of the portable device for DNA amplification and detection. The uMED^{NA} is connected to the heating module. A test strip is shown on top of the planar heating mat.



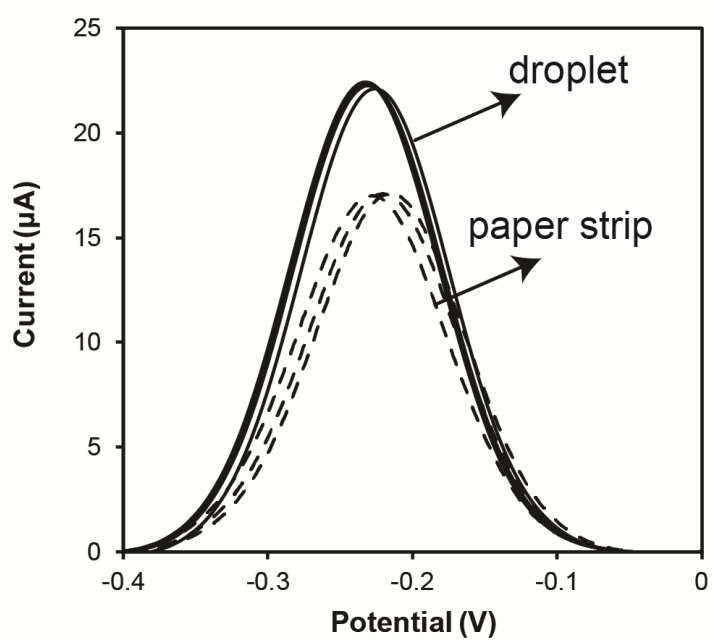
SI Figure 4: Circuit diagram for the heating module of the uMED^{NA} portable device.



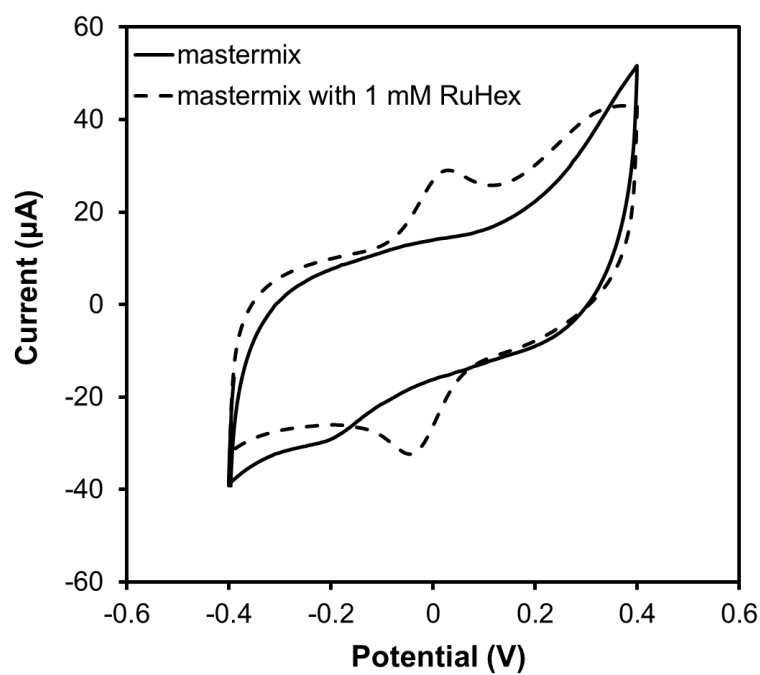
SI Figure 5: Plots of the anodic peak current (i_{pa}) and cathodic peak (i_{pc}) current as a function of the concentration of electroactive mediator $[\text{Ru}(\text{NH}_3)_6]^{3+}$ from cyclic voltammograms collected on the uMED^{NA}. Data for i_{pa} and i_{pc} are shown in filled and unfilled black squares, respectively, including trendlines and R-squared values.



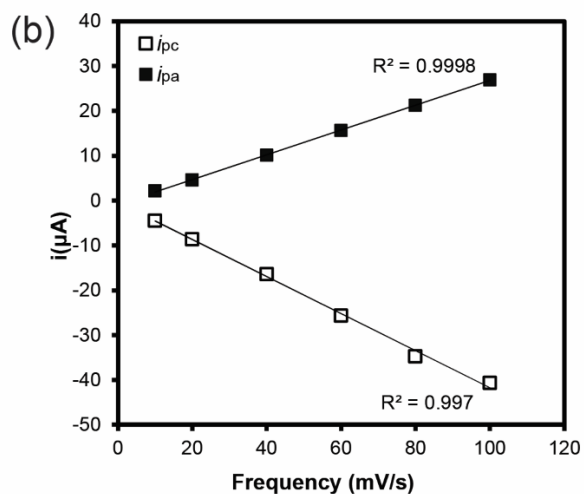
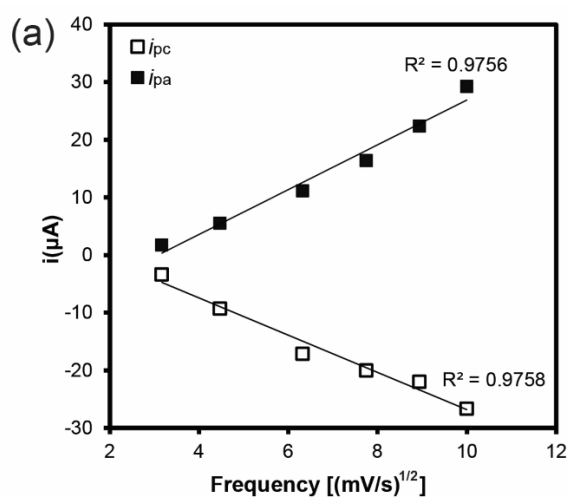
SI Figure 6: Electroanalytical results on the uMED^{NA} portable device. Square-wave voltammograms (n=3, 50 μ L, 14.7 Hz frequency, 50 mV amplitude, and 50 mV/s scan rate) of 250 μ M $[\text{Ru}(\text{NH}_3)_6]^{3+}$ in Tris-acetate buffer (40 mM, pH 7.4) measured in a liquid droplet on a bare SPE or on a disposable paper-based test strip.



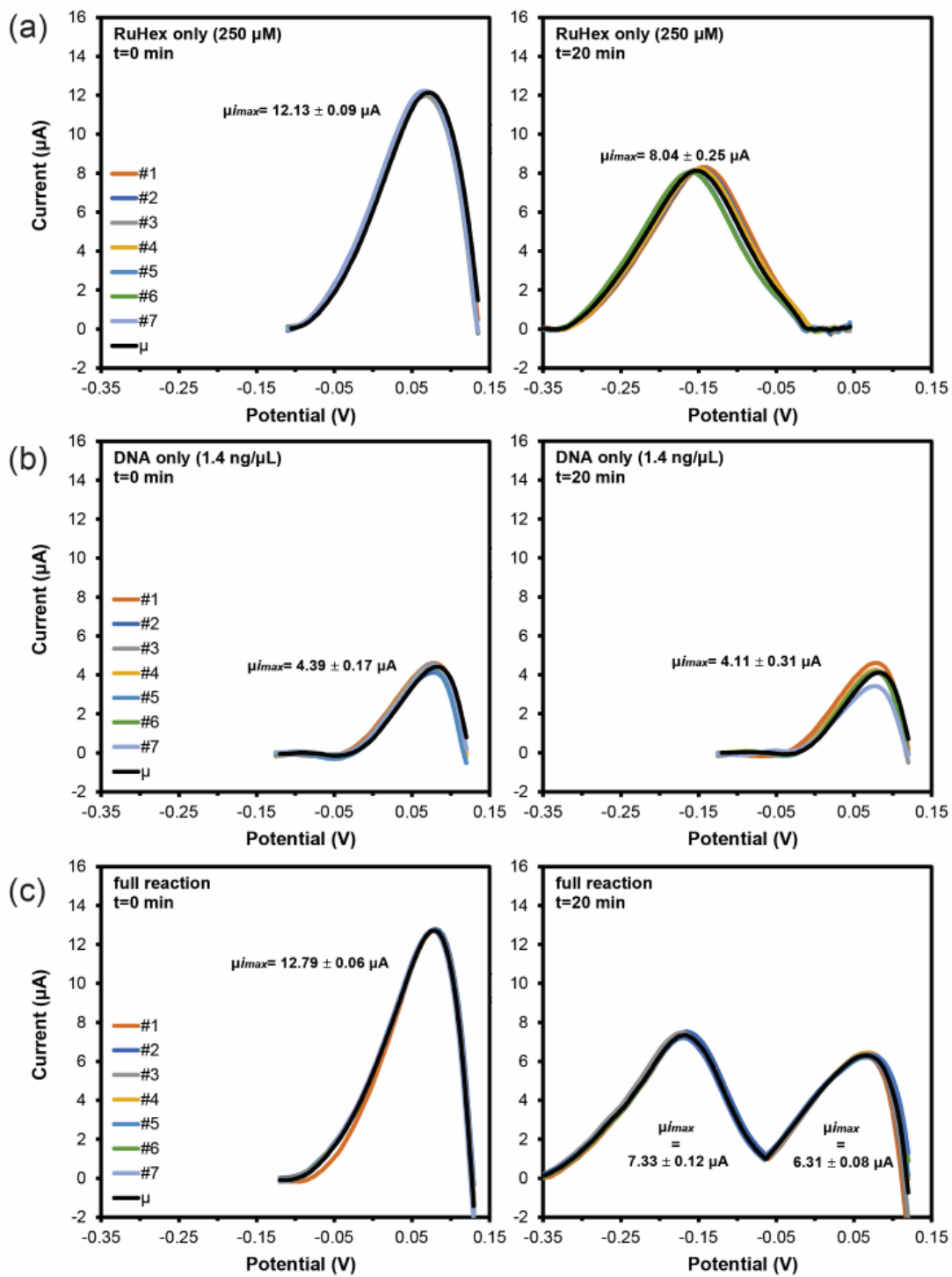
SI Figure 7: Cyclic voltammograms collected on the uMED^{NA} portable device (50 mV/s scan rate) of the RPA mastermix in the absence and presence of 1 mM [Ru(NH₃)₆]³⁺. Data from in the absence and presence of mediator are depicted with a dashed and solid line, respectively.



SI Figure 8: Studies of the cyclic voltammograms at different scan rates (10, 20, 40, 60, 80 and 100 mV/s on the uMED^{NA} portable device using paper-based test strips at t=0 and t=20 minutes of the RPA reaction (25 μ L, 15 Hz frequency, 50 mV amplitude, and 50 mV/s scan rate). (a) Results for peak current I_p at=0 min confirm a diffusional process. (b) Results for peak current I_p at=20 min confirm a surface-confined process.



SI Figure 9: Square-wave voltammograms collected on the uMED^{NA} portable device using paper-based test strips at t=0 and t=20 minutes of the RPA reaction (25 μ L, 15 Hz frequency, 50 mV amplitude, and 50 mV/s scan rate). The same potential range was scanned for [Ru(NH₃)₆]³⁺ only (a), DNA only (b), and [Ru(NH₃)₆]³⁺ with DNA (c). We performed experiments in n=7 replicates, containing the components of the full reaction, prepared independently. The black line denotes the arithmetic mean of the seven replicate experiments.



Supporting Tables

Table 1: The sequences of the primers and target DNA used in the RPA assay. The target DNA sequence is a 213-nucleotide region within the 16S rRNA sequence of genus *Mycobacterium* of 16S rRNA *M. smegmatis* gene (GenBank X52922.1).

Name	DNA Sequence
Forward primer	5'-TGA GTA ACA CGT GGG TGA TCT GCC CTG CAC TTT GG-3'
Reverse primer	5'-AGT CCC AGT GTG GCC GGT CAC CCT CTC AGG CCG GC-3'
Target sequence	5'-TGA GTA ACA CGT GGG TGA TCT GCC CTG CAC TTT GGG ATA AGC CTG GGA AAC TGG GTC TAA TAC CGA ATA CAC CCT GCT GGT CGC ATG GCC TGG TAG GGG AAA GCT TTT GCG GTG TGG GAT GGG CCC GCG GCC TAT CAG CTT GTT GGT GGG GTG ATG GCC TAC CAA GGC GAC GAC GGG TAG CCG GCC TGA GAG GGT GAC CGG CCA CAC TGG GAC T-3'

Supporting References

- [1] T. Notomi, H. Okayama, H. Masubuchi, T. Yonekawa, K. Watanabe, N. Amino, T. Hase, *Nucleic Acids Res.* 2000, 28, e63-e63.
- [2] J. Compton, *Nature* 1991, 350, 91-92.
- [3] M. Vincent, Y. Xu, H. Kong, *EMBO Rep.* 2004, 5, 795-800.
- [4] A. J. Bard, L. R. Faulkner, *Electrochemical Methods: Fundamentals and Applications*, Vol. 2, Wiley New York, 1980.
- [5] A. Bejan, I. Dincer, S. Lorente, A. Miguel, H. Reis, *Porous and complex flow structures in modern technologies*, Springer Science & Business Media, Cambridge, MA, USA, 2013.
- [6] E. M. Renkin, *J. Gen. Physiol* 1954, 38, 225-243.
- [7] C. D. Shackelford, D. E. Daniel, *J. Geotech. Eng.* 1991, 117, 467-484.
- [8] B. V. Slaughter, S. S. Khurshid, O. Z. Fisher, A. Khademhosseini, N. A. Peppas, *Adv. Mater.* 2009, 21, 3307-3329.
- [9] T. Rogall, J. Wolters, T. Flohr, E. C. Bottger, *Int. J. Syst. Bacteriol.* 1990, 40, 323-330.
- [10] R. Kalendar, D. Lee, A. H. Schulman, *Genomics* 2011, 98, 137-144.